A multimode electromechanical parametric resonator array

Supplementary Information

I. Mahboob, M. Mounaix, K. Nishiguchi, A. Fujiwara and H. Yamaguchi

NTT Basic Research Laboratories, NTT Corporation, Atsugi-shi, Kanagawa 243-0198, Japan

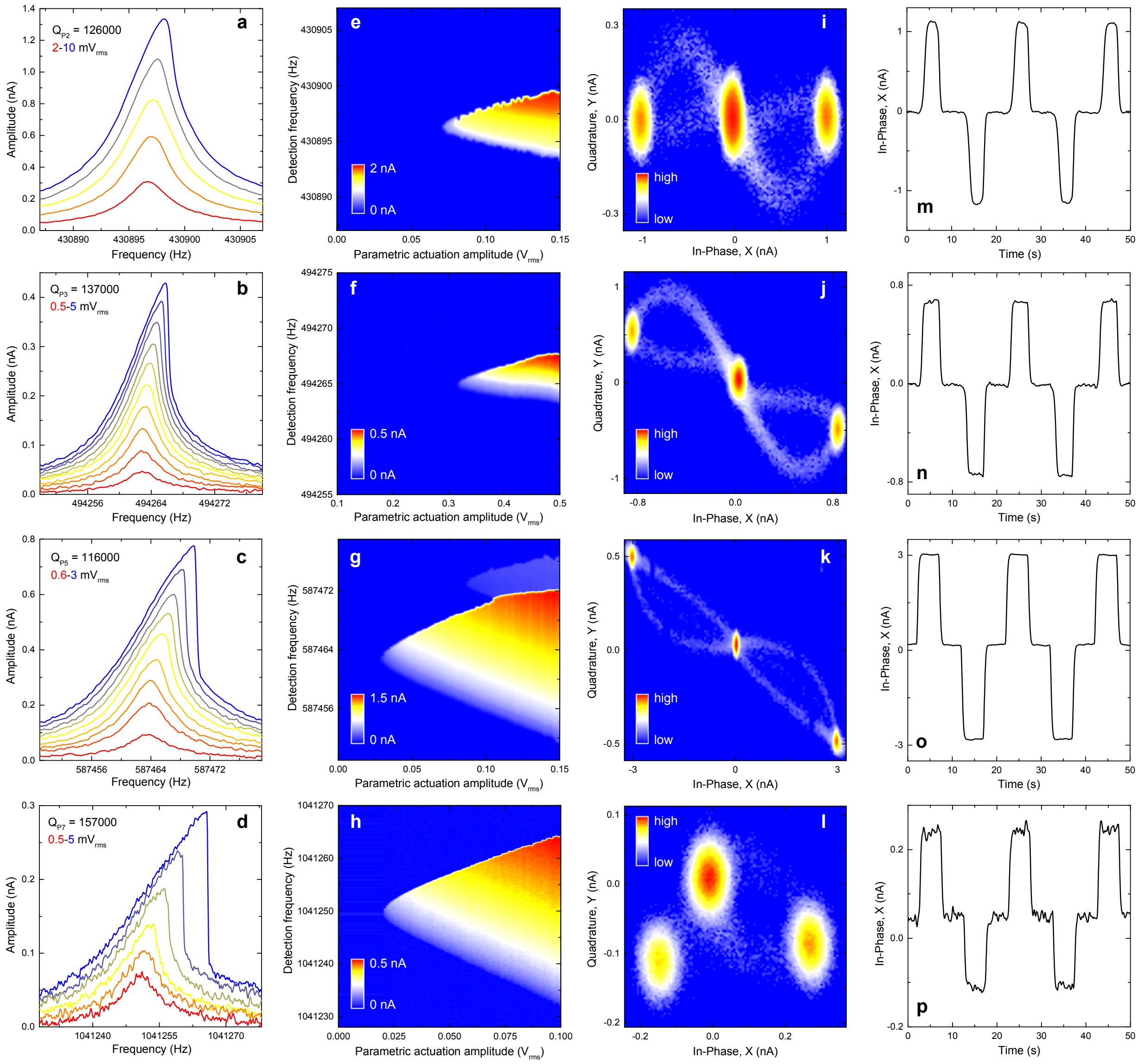

Supplementary Figure S1: **The harmonic and parametric resonance dynamics of modes P2, P3, P5 and P7. a-d,** The harmonic response of modes P2, P3, P5 and P6 as a function of actuation amplitude. **e-h,** The parametric response of the same modes as a function of the actuation amplitude measured in a subharmonic detection configuration. **i-l,** The stability diagrams indicate the occupation probabilities of the parametric resonances in phase space and are measured with parametric actuation amplitudes and frequencies of 0.12 V_{rms} and 861793 Hz, 0.5 V_{rms} and 988532 Hz, 0.2 V_{rms} and 1174926 Hz, 0.15 V_{rms} and 2082500 Hz for modes P2, P3, P5 and P7 respectively. **m-p,** Using the pulse sequence outlined in Fig. 1c, binary information can be written, stored and erased in the bi-stable oscillation phases of the parametric modes at the above quoted actuation amplitudes and frequencies.

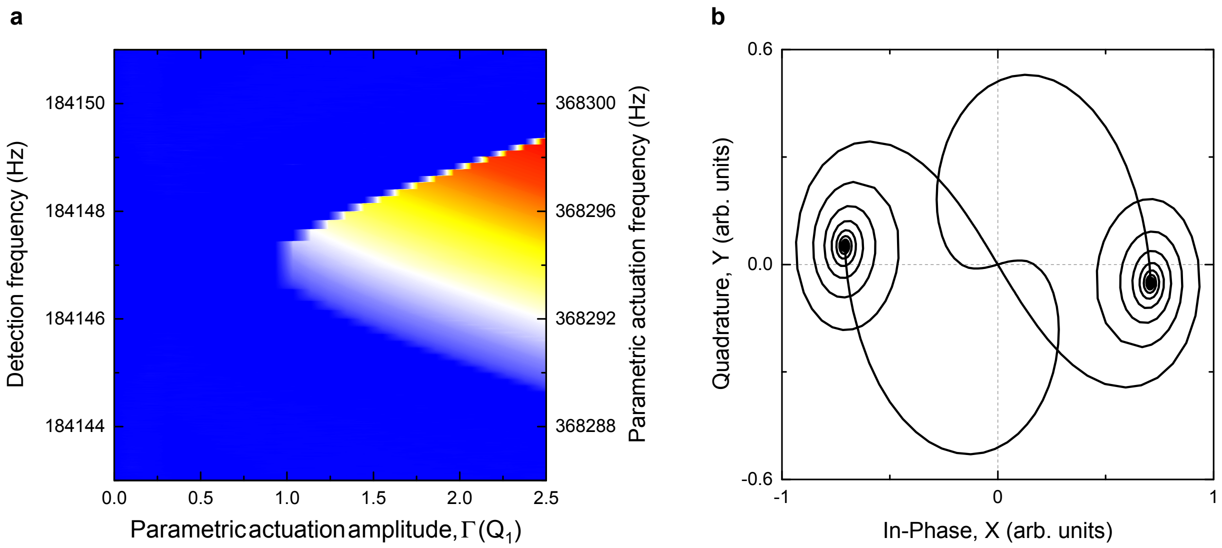

Supplementary Figure S2: **Solutions to Mathieu's equation for mode P1.** **a**, Mathieu's equation (described in the main text) is numerically solved as described in ref. 20 for mode P1 as a function of the parametric actuation amplitude and frequency where the onset of parametric resonance is defined by the condition $\Gamma = Q_{P1}$ [20]. **b**, Mathieu's equation is also solved exactly on resonance with an amplitude that is 7 times the threshold to parametric resonance in order to extract the temporal evolution of the in-phase and quadrature components of mode P1's position. This calculation reveals that if the initial, i.e. at time $t = 0$, in-phase component is positive (negative) then it evolves to a state with positive (negative) in-phase component upon parametric excitation with a trajectory that reproduces the experimentally observed response shown in Fig. 1g. More fundamentally, the solutions to Mathieu's equation enable the higher order parametric resonance modes to be evaluated with the benchmark provided by the P1 mode in order to confirm their parametric resonance dynamics.

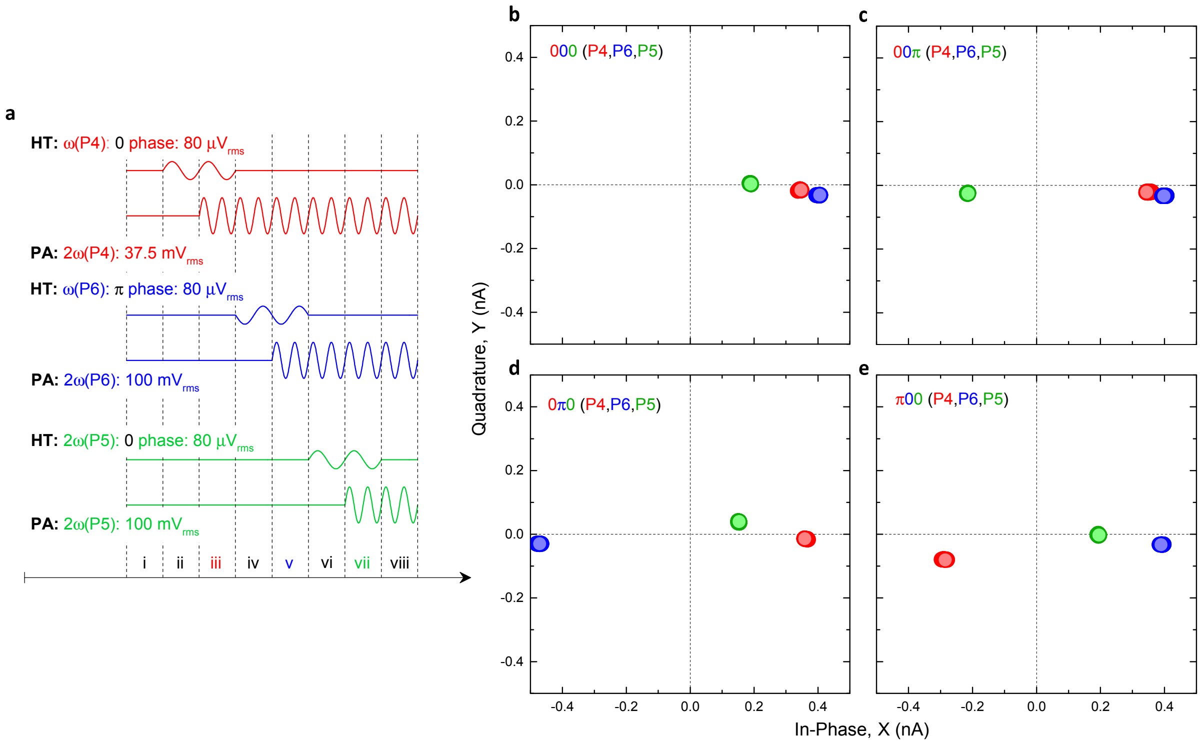

Supplementary Figure S3: **An electromechanical 3-bit byte.** **a**, The pulse sequence used to execute a 3-bit byte where the harmonic trigger excitation enables the $0/\pi$ logical to be written into the phases of modes P4, P6 and P5 when they are parametrically excited in parallel namely steps iii, v and vii. Deactivating the trigger whilst the parametric actuation remains active enables this information to be stored as depicted in steps iv, vi and viii. The pulse sequence shown enables the string $0\pi0$ to be written. **b-e**, The response of modes P4, P6 and P5, when subjected to the above sequence on resonance with the measured outputs projected in phase space. The 3-bit byte has 8 combinations, but only the 000, 00π, $0\pi0$ and $\pi00$ configurations are shown based on symmetry considerations where the 1^{st}, 2^{nd} and 3^{rd} logicals are encoded in modes P4, P6 and P5 respectively with the positive (negative) in-phase component corresponding to the binary logical 0 (π). The phase portraits confirm the successful execution of the 3-bit byte where the responses of modes P4, P6 and P5 are broadened due to the 3 modes being repeatedly sampled on resonance.

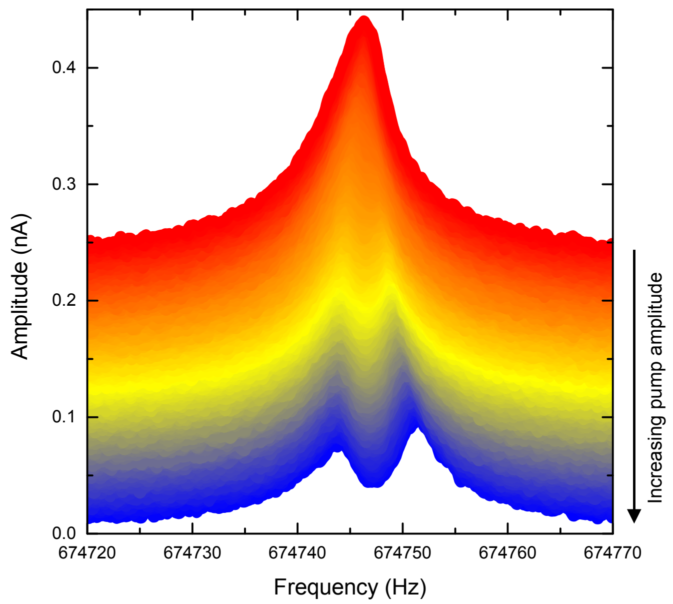

Supplementary Figure S4: **Dynamic coupling between elements of the electromechanical parametric resonator array.** Mode P6 is harmonically probed with an actuation amplitude of 1 mV_{rms} in the presence of the parametric coupling pump at the frequency difference to mode P4, see schematic in Fig. 4a, as its amplitude is increased from 0 to 1.5 V_{rms}. With increasing pump amplitude, the sideband from mode P6 increasingly overlaps with mode P4 and vice versa resulting in modes P6 and P4 coupling ever more strongly until they hybridise and undergo parametric normal mode splitting. This measurement confirms that elements of the electromechanical parametric resonator array can be selectively and controllably be coupled and it forms the basis of the electromechanical shift register and the inverter logic gate.

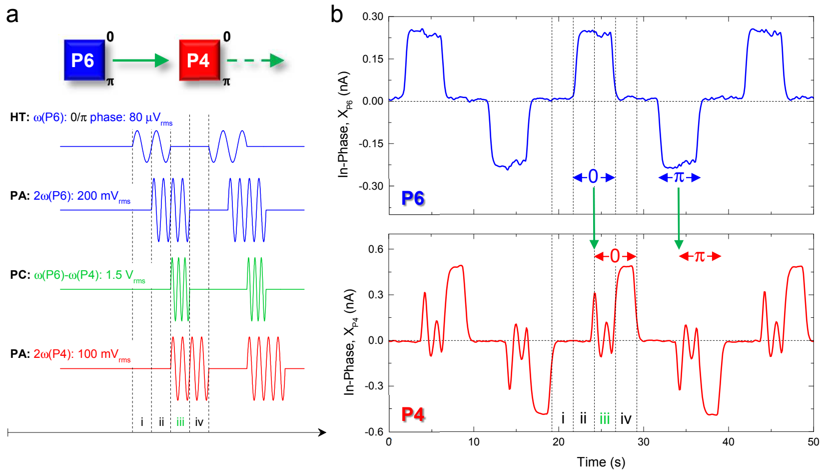

Supplementary Figure S5: **Reversible phase information transfer in the electromechanical parametric resonator array. a** , The block diagram summarising the corresponding pulse sequence used to implement phase information transfer between modes P6 and P4 namely in reverse to the sequence detailed and executed in Figs. 4b and 4c. **c**, Implementation of the pulse sequence described in Fig. S5a where the positive/negative polarity of the in-phase component of the parametric resonances corresponding to logical $0/\pi$ is conserved during transmission between the modes. Note also that when the parametric coupling pump is activated in step iii, the parametric resonance of mode P4 fluctuates during the information transfer. This measurement confirms that phase information can be readily shifted in both directions in the electromechanical parametric resonator array without the need for hardware rewiring.

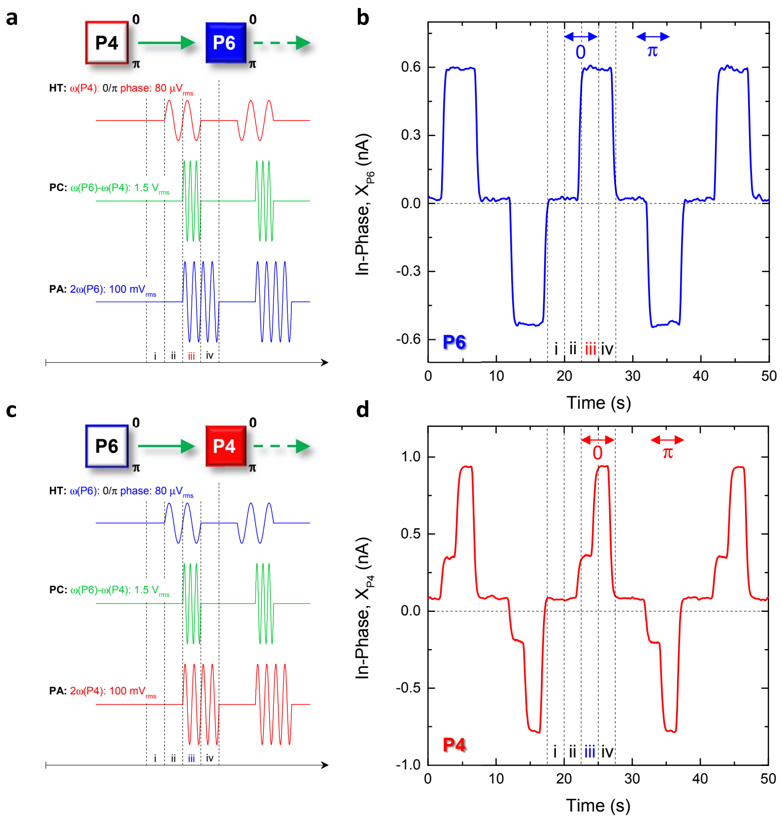

Supplementary Figure S6: **Phase shift in the electromechanical parametric resonator array. a** (**c**), Before the shift register could be implemented, the possibility of the oscillation phase of one mode triggering the parametric oscillation phase of another mode was investigated in the electromechanical parametric resonator array. The system is first initialised by its stationary state in step i. Next mode P4 (P6) is harmonically triggered with a 0 phase oscillation (step ii) followed by the simultaneous activation of parametric coupling and the parametric actuation of mode P6 (P4) in step iii. Activation of the parametric coupling pump results in modes P4 and P6 hybridising (as depicted in Fig. S4) thus enabling information to be exchanged between them. The phase information transmitted to mode P6 (P4) can then be stored via its parametric resonance in step iv. This protocol is then repeatedly cycled with a π phase and 0 phase trigger as summarised in the block diagram where the open (filled) box indicates harmonic (parametric) actuation of a mode. **b** (**d**), Implementation of this protocol whilst observing the in-phase oscillation component of mode P6 (P4) confirms that phase information can successfully be transmitted between the elements of the electromechanical parametric resonator array. Note also that in step iii in Fig. S6d, the simultaneous activation of the harmonic trigger in mode P6 and the parametric coupling pump modifies the output of mode P4. This effect is further amplified when the weak harmonic triggering of mode P6 is replaced by its parametric resonance in the shift register as shown in step iii in Fig. S5b.

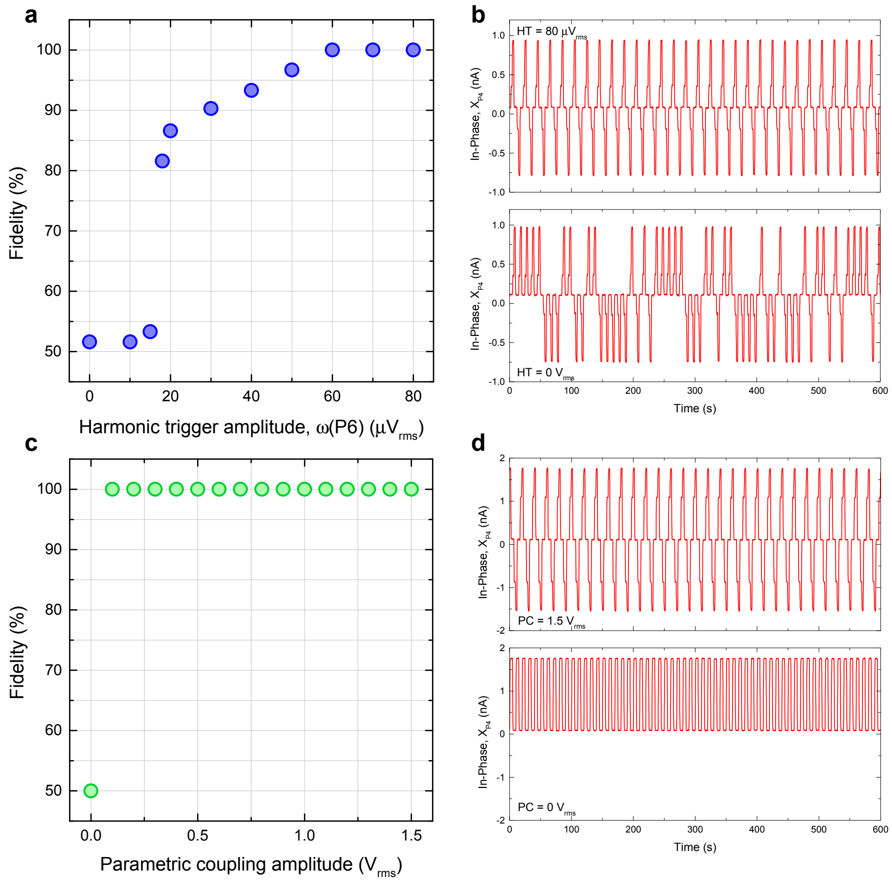

Supplementary Figure S7: **Fidelity of the phase shift protocol in the electromechanical parametric resonator array.** The fidelity of the phase shift protocol described in Fig. S6c is investigated as a function of **a**, the harmonic trigger amplitude of mode P6 and **c**, the parametric coupling pump amplitude. **b**, For mode P6 harmonic trigger amplitudes of $\geq$ (<) 60 mV$_{rms}$, the output from mode P4 shown in the upper (lower) panel reveals sequential (random) switching between the 0 phase oscillation and the π phase oscillation as expected from the pulse sequence described in Fig. S6c. **d**, On the other hand, if the parametric coupling pump is operated with amplitudes of ≥ 0.1 V$_{rms}$, phase information can successfully be transferred from mode P6 to mode P4 with 100% fidelity resulting in the expected periodic switching in the oscillation phase of mode P4. Consequently, this result indicates that even weak coupling is sufficient to transfer phase information between the elements of the electromechanical parametric resonator array.

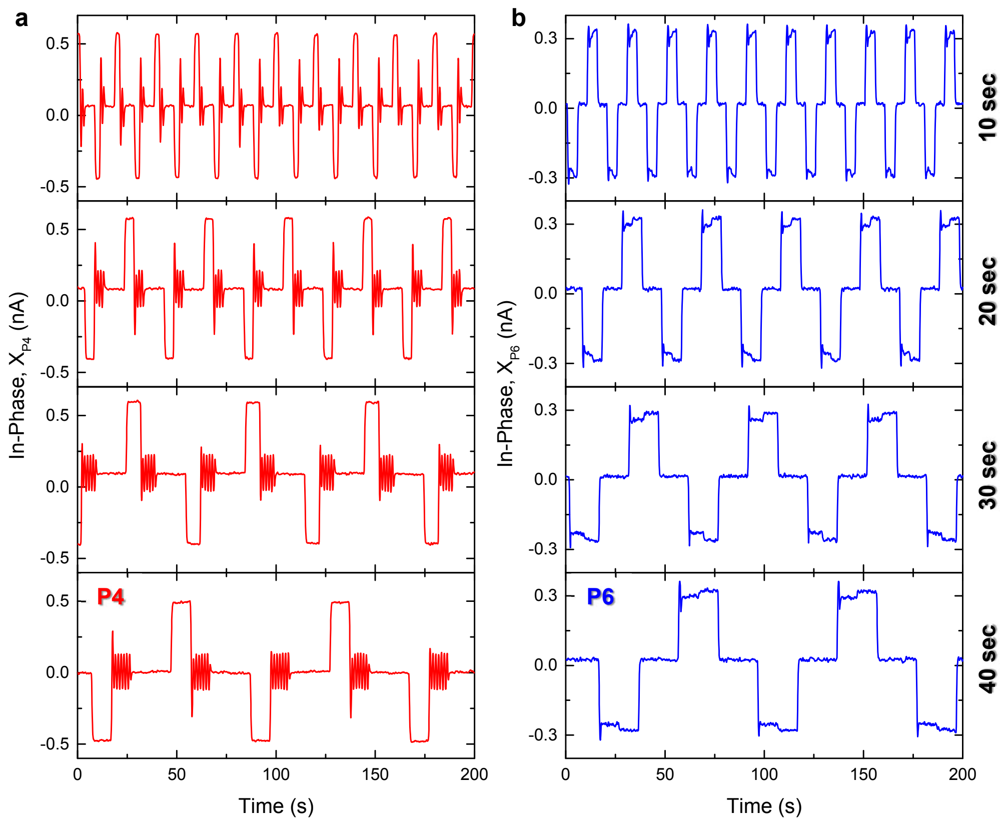

Supplementary Figure S8: **Temporal control of phase information in the electromechanical parametric resonator array.** The pulse sequence shown in Fig. 4b can also be implemented by varying the time period given by the sum of steps i to iv from 10, 20, 30 and 40 seconds and is confirmed by measuring the resultant in-phase components of the vibration from **a**, mode P4 and **b**, mode P6 in parallel.